Numerical Investigations of a Large Scale Pressure Vessel Test

Arja Saarenheimo, Heli Talja, Kari Ikonen
VTT, Nuclear Engineering Labortory, Helsinki, Finland
Rauno Rintamaa, Heikki Keinänen, Kari R. Törrönen
VTT, Metals Laboratory, Espoo, Finland

ABSTRACT

Numerical methods for fracture assessments are verified by the experimental findings of the hydrotest with a large size pressure vessel, the dimensions of which resembled those of a nuclear reactor pressure vessel. For fracture mechanics considerations, a sharp artificial axial surface flaw was made on the inner wall of the vessel. One of the circumferential welds of the vessel intersected the crack at its midpoint, which caused the premature failure of the vessel as a local rupture of the crack ligament. Two- and three-dimensional elastic-plastic FE-analyses were carried out. For fracture mechanics evaluation J-integrals along the crack front and along the front of the local leak were calculated. The amount of the stable crack growth and the fracture behaviour were assessed based on the calculated J-variations and the measured J_R-curves. Calculated and measured values are presented in this paper.

1 DESCRIPTION OF THE PRESSURE VESSEL TEST

The destructive hydrotest was carried out with a large retired pressure vessel (outer diameter 2885 mm, length about 16 m), which was used as a hydrogen cracking reactor in Neste Oy's oil refinery plant for nearly 20 years. The design pressure and temperature were 144 bar and 471 °C. The wall thickness of the cylindrical part was 152 mm. A sharp artificial axial flaw with a length of 2520 mm and depth of 100 mm was made into the inner wall of the vessel. One of the circumferential welds of the vessel located in the half-way of the crack length (Fig. 1). A maintenance deck, which was located around the mid section of the pressure vessel, was partially removed so as to prevent the interference with the expected vessel deformations upon pressurization. Ovalizations, crack field strains and crack mouth opening were measured in the test. Additionally, fracture behaviour was monitored by acoustic emission measurements.

The vessel was pressurized up to failure by water in the temperature of 60 °C. When a pressure value of 170 bar was reached, a local leak occurred in the circumferential weld crossing the flaw. The pressure could be increased up to 186 bar, at which pressure the leak rate overcame the capacity of the pumps. More detailed description of the experimental results has been presented in /2/.

2 NUMERICAL SIMULATION

Elastic-plastic and geometrically nonlinear finite element analyses were carried out using the 84-

version of the ADINA /1/ code in a CDC CYBER 180/840 computer. The J-integral values were calculated by applying the deLorenzi formulation of the virtual crack extension (VCE) method and using a post-processor program VTTVIRT /3/. The correction term due to pressure on the crack surfaces was taken into account.

Due to the geometry of the flaw, three-dimensional effects were essential. Because of two symmetry planes, only one quarter of the pressure vessel had to be modeled Fig. 2. Further the length of the model was limited to 3.5 m in the axial direction because the influence of the crack was assumed to be local in the axial direction. Axial displacements at the end of the model were forced to be equal to the displacements caused by pressure in an unflawed vessel.

The model shown in Fig. 2 contained about 6000 nodal points and the total number of degrees of freedom was over 16000. There were 1000 20-noded and 100 15-noded three-dimensional volume elements and one beam element with cross section of 50x300 mm^2. This was needed to describe the effect of the maintenance deck. A detail of the mesh near the artificial flaw is shown in Fig. 3. The crack tip was modeled by collapsed elements causing an 1/r-singularity in the strains near the crack front. Two different analyses with stationary cracks were carried out. The aim of the first one with original crack geometry, was to locate where the crack starts to grow and to estimate the amount of the stable crack growth along the crack front. The aim of the second analysis with the through-the-wall crack geometry, was to study whether the narrow through-the-wall crack tends to grow in the axial direction, i.e. into the base metal. For the second analysis the finite element model was modified. Circumferential displacements were released at the surface of the through-the-wall crack. Possible overlapping along crack surfaces was prevented through the use of gap elements. No initial deformations were imposed. The equilibrium equations were solved by the Newtons iteration method combined with a line search method. In the first three-dimensional analysis 112 h cpu-time was used and in the second 125 h.

The different material properties of the base and weld materials were taken into account. The yield stress for the weld material was 346 N/mm^2 and 258 N/mm^2 for the base material. The ultimate stress values were 530 N/mm^2 and 500N/mm^2, respectively. The crack growth resistance curves (J_R-curves) of both metals are shown in Fig 4. Fracture resistance was much higher for the base material than for the weld material. The J_{1C}-values of the base and weld materials were 378 kN/m and 70 kN/m, respectively.

3 RESULTS AND DISCUSSION

Because of the flaw, the vessel wall was subjected to bending. The flaw deflected to the inside of the vessel as shown in Fig. 2. The measured and calculated diameter changes are presented in Fig. 5. The diameter as measured parallel to the crack decreased while the diameter measured perpendicular to the crack plane increased. Calculated changes of diameter were somewhat larger than the measured ones. The difference between two- and three-dimensional results was relatively small. The reason for that was presumably the stiffening effect of the maintenance deck.

Hoop strains along the outer and inner surfaces of the vessel circumference at one third of the crack length are presented as functions of the pressure in Figs. 6 and 7. The strains calculated with a three-dimensional model agreed well with the measured ones. Measured and calculated hoop strains along the inner surface were higher than those along the outer surface at 90^0. At 45^0, however, the situation was reversed indicating significant influence of the crack on the stress field.

Comparison of calculated and measured hoop strains adjacent to a crack cross-section (1/4 crack length position) is presented in Fig 8. The hoop strain (K22) in the ligament just opposite to the crack tip was compressive reaching the minimum value in the pressure range from 120 bar to 140 bar. The measured and calculated strains had a similar trend, but there were some differences between the absolute values. Near the ligament, the outer surface hoop strains had a high gradient as a function of the distance from the crack plane, hence small inaccuracies in gage locations may be one reason for the differences between calculated and measured strains.

The measured and calculated crack mouth opening (COD) values at one quarter of the crack length are presented in Fig. 9 as function of the pressure. The agreement between measured and calculated COD-values was good. Calculated crack tip opening values, which are taken as crack tip node displacements (CTOD) are also shown in Fig. 9. The CTOD value corresponding to the J_{1c} value of the base material was about 0.7 mm, which was reached at a pressure of 150 bar.

The J-integral values were calculated as a mean value from three successive element rings. The finite element model contained four elements through the ligament. The J-values along the crack front are presented in Fig. 10 at pressures of 50, 100, 150, 185 and 190 bar. The maximum J-value occurred in the weld and was about 10% higher than the corresponding value in the neighbouring base material. The deformations of the narrow weld area were forced to be equal to those of the base material. The higher yield strength of the weld material caused higher J-integral values in the weld. The J_{1c} value of 70 kN/m was reached in the weldment already at the pressure of 75 bar. In the base material, close to the weld, the J_{1c} value of 378 kN/m was reached at 150 bar.

On the basis of the material J_R-curve and the calculated J-values one can estimate stable crack growth at the end of the test (186 bar). In the base material, the estimated crack growth is 3.5 mm in the vicinity of the weld, at the quarter position of crack length 2.5 mm, and at the crack's end no crack growth in axial direction is expected. Fracture surface investigations indicated about 2 mm crack growth over a length of approximately 150 mm on both sides of the leak. However, the J-level in the weld is much higher than the J_R-curve values, which could indicate instability or at least considerable crack growth through the weld. Estimated and measured crack growths are compared in Fig. 12.

During the test, when the pressure reached a value of 130 bar, a noise was heard indicating a pop-in type crack extension, which was confirmed by fracture surface investigations. After the 'pop-in' in the weld area the crack growth stopped when the ligament thickness was only a few millimeters. The crack arrest was presumably caused by compressive hoop stresses acting near the outer surface. This is consistent with the results of the second part of the finite element analysis where the through-the-wall crack did not start to open before the pressure value of 150 bar was reached.

This occurrence can also be seen through J-integral values calculated along the front of the narrow through-the-wall crack. Fig. 11 shows the J-integral values along the new front at pressure values 50, 100, 150, 185 and 190 bar. A very sharp peak in the J-distribution occurred in the crossing of the unburst and new crack fronts. It can partly be caused by numerical effects but nevertheless, it shows that the through-the-wall crack tends to grow much faster near the inner surface, where it should extend considerably into the base material. This is also supported by the shape of the experimental through-the-wall crack (Fig. 12). After the test the width of the opening was at the inner surface 100 mm and only 25 mm at the outer surface, where also the J-integral was low. Presumably the crack growth near the weld has mostly taken place after the pop-in occurrence (appr. 130 bar).

4 SUMMARY AND CONCLUSIONS

A destructive pressure test with a large flawed vessel was investigated by using two- and three-dimensional finite element models. Two three-dimensional analyses were performed. In the first one, the axial surface flaw was modeled allowing for different stress-strain curves of the base and weld material. In the second analysis, one of the circumferential welds of the vessel intersecting the axial surface flaw at its midpoint and causing a local rupture of the flaw ligament during the hydrotest, the model included a narrow through-the-ligament crack.

Calculated diameter changes of the pressure vessel, the crack mouth opening displacements and far-field and crack field strains were compared with the measured values. The flawed region collapsed slightly inward and compressive strains and stresses occurred in the outer surface of the vessel. Calculated changes of the diameter, COD and strain values based on the three-dimensional analysis showed an good agreement with the measured ones.

For fracture behaviour assessment of the pressure vessel J-integral values were calculated along the unburst crack front. In the middle of the crack length J-values were considerably higher than at the ends indicating crack growth only in the through-the-thickness direction. Due to the higher yield stress of the weld material, the J-values in the weld were about 10% higher than in the neighbouring base material. The higher J-value combined with the low ductility of the weld material explains why the crack penetrated through the wall only in a narrow region flaw ligament, where the circumferential weld located. The amount of stable crack growth was slightly overestimated by the calculation. According to the calculations crack growth should have been initiated in the weldment region at the pressure of 75 bar. This value is somewhat conservative in that a pop-in type crack extension occurred at a pressure of 130 bar during the experiment.

In the second analysis, a small through-the-wall crack was included in the model. The J-variation in this crack front explains the crack shape. At the point of intersection of the original flaw and the through-the-wall crack front, a pronounced maximum is seen in the J-integrals. Small values at the outer surface are consistent with the negative hoop stresses and indicate that the crack tends to open at the surface only at a high pressure level. Thus the pop-in type crack growth almost through the weld can be understood.

If the crack had been located entirely in the base material, it would have presumably penetrated the wall along most of its length thus causing a catastrophic failure. The failure pressure would probably have been slightly over 200 bar.

Though the complicated geometry, the overall agreement between experimental and calculated displacement and strain results was good. Conservative estimates were obtained for stable crack growth. Extensive three-dimensional analyses were necessary to explain the failure behaviour in the test.

ACKNOWLEDGEMENTS

The work was carried out as a part of the project "Prevention of catastrophic failure of pressure vessels and piping", which is a part of the Nordic co-operative project "Elastic-plastic fracture mechanics". The Nordic project is carried out under the auspices of the Nordic Liaison Committee of Atomic Energy. The financing of the research reported here was obtained from the Nordic Council of Ministers, Centre for Radiation Protection and Nuclear Safety in Finland, Swedish Nuclear Power Inspectorate, Technology Development Centre of Finland, Ministry of Trade and Industry in Finland, Technical Research Centre of Finland, Neste Oy, Imatra Power Co and Oy Huber Ab.

REFERENCES

/1/ ADINA, 1984. ADINA-automatic dynamic incremental nonlinear analysis. ADINA Engineering AB, Västerås, 1984. Report AE 84-1.

/2/ Rintamaa et. al., Fracture behaviour of large scale pressure vessels in the hydrotest. Int. J. Pres. Ves. & Piping 34 (1988) 265-291.

/3/ Talja, H., Calculation of elastic-plastic fracture mechanics parameters by using the finite element method. Espoo 1987. 113p (in Finnish).

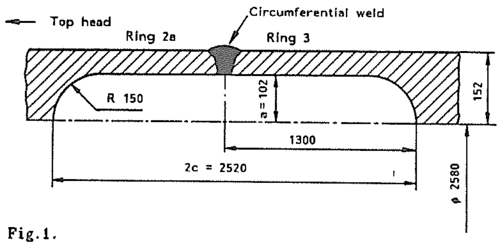

Fig.1.

Dimensions and geometry of the axial flaw produced into the inner wall of the vessel.

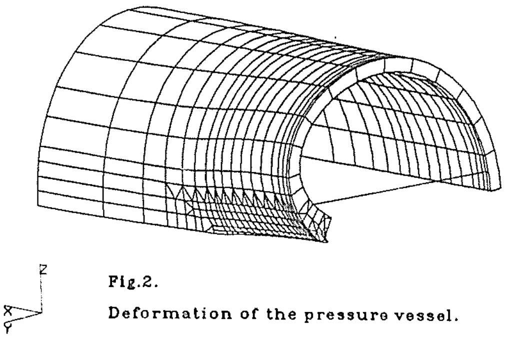

Fig.2.

Deformation of the pressure vessel.

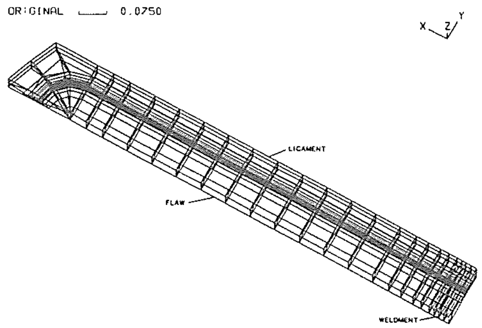

Fig.3.

Part of the 3D FE model for the evaluation of weldment behaviour in the flaw ligament.

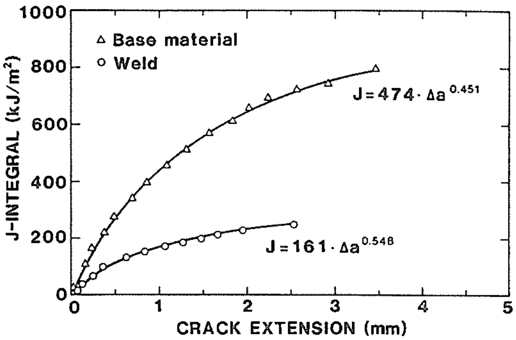

Fig.4.

Fracture recistance curves for base and weld material determined at 80°C.

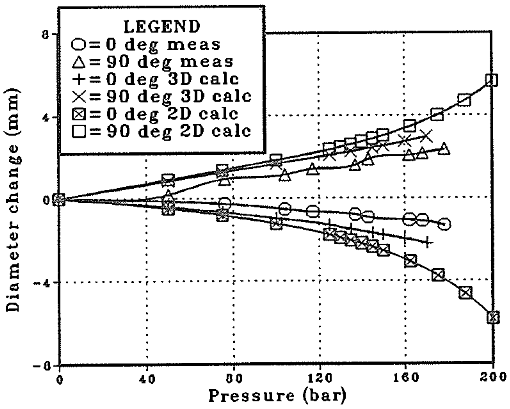

Fig.5.

Calculated and measured diameter changes of the pressure vessel parallel (0deg) and perpendicular (90deg) to the crack plane.

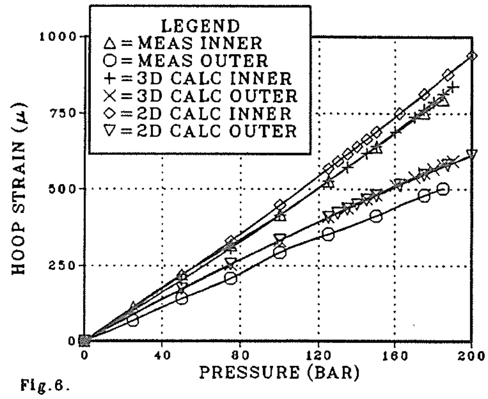

Fig.6.

Calculated and measured inner surface and outer surface hoop strains along the pressure vessel circumference at the orientation of 45deg and crossing the crack ligament at one third of the crack length.

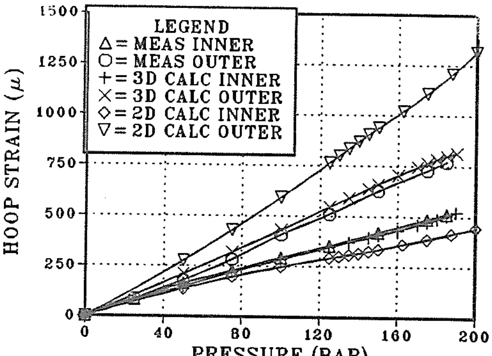

Fig.7.

Calculated and measured inner surface and outer surface hoop strains along the pressure vessel circumference at the orientation of 90deg and crossing the crack ligament at one third of the crack lenght.

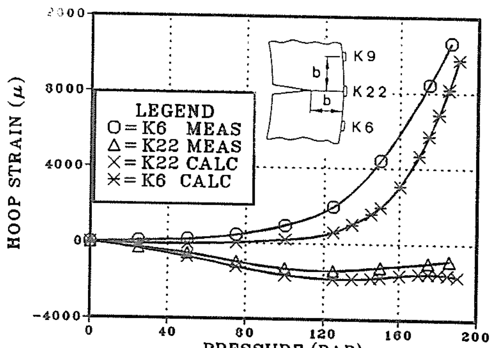

Fig.8.

Calculated and measured outer surface surface hoop strains of the ligament cross-plane located at the 1/4 crack length.

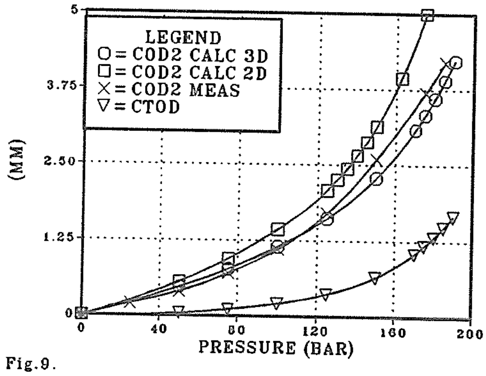

Fig.9.

Calculated and measured crack mouth opening displacements at the 1/4 (COD2) of the crack lenght as well as calculated crack tip opening displacement (CTOD) at the COD2 position.

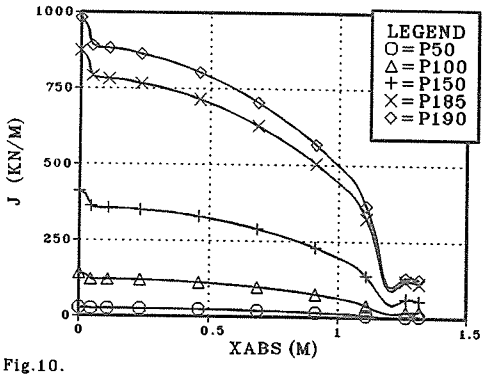

Fig.10.

Distribution of the J-integral value along the surface crack front at different pressure levels.

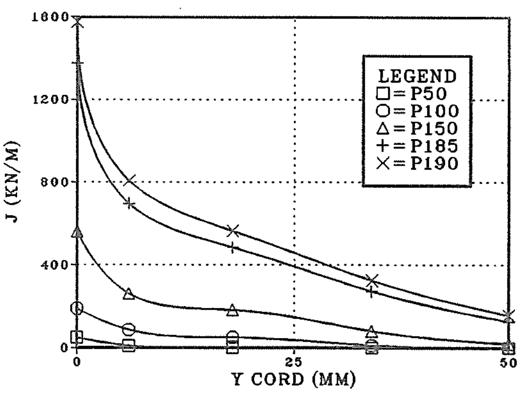

Fig.11.

Distribution of the mean J-integral value along the through-the-wall crack front.

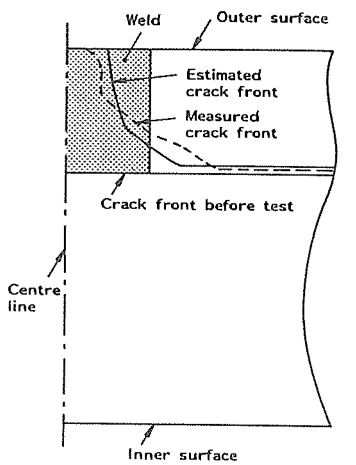

Fig.12.

Estimated and measured crack front location in the local leak region.